We are IntechOpen, the world's leading publisher of Open Access books Built by scientists, for scientists

6,900
Open access books available

185,000
International authors and editors

200M
Downloads

Our authors are among the

154
Countries delivered to

TOP 1%
most cited scientists

12.2%
Contributors from top 500 universities

CLARIVATE ANALYTICS

BOOK CITATION INDEX

INDEXED

WEB OF SCIENCE™

Selection of our books indexed in the Book Citation Index
in Web of Science™ Core Collection (BKCI)

Interested in publishing with us?
Contact book.department@intechopen.com

Numbers displayed above are based on latest data collected.
For more information visit www.intechopen.com

Electrical Properties of Polymer Light-Emitting Devices

Lucas Fugikawa Santos and Giovani Gozzi

Additional information is available at the end of the chapter

Abstract

In this chapter, we present a brief introduction to semiconducting properties of conjugated polymers and the motivation to apply this class of materials in electronic/optoelectronic devices such as polymer light-emitting diodes (PLEDs). We describe, in detail, the operating mechanisms of PLEDs, with particular focus on the effects of charge injection and transport and their dependence on the external electric field and temperature. The mechanisms of current injection from the electrodes into the organic semiconductor are initially treated using traditional models for thermionic emission and tunnelling injection. More recent models considering the influence of metal/semiconductor interface recombination and of energetic and spatial disorder in the injection currents are also introduced and discussed. In addition, models considering space-charge-limited currents and trap-filling-limited currents are employed to describe the charge transport characteristics in the bulk. Furthermore, we present a brief discussion on ideas concerning the effects of the disorder on the charge-carrier transport behaviour.

Keywords: polymer light-emitting diodes, conjugated polymers, electrical properties, space-charge-limited currents, organic semiconductors

1. Introduction

In the past three decades, we have witnessed an impressive fast-growing number of scientific publications concerning the electronic and optoelectronic properties of semiconducting polymers, from fundamental theoretical studies to reports of cutting-edge applications. In the same period, the device performance, quantified by device parameters such as charge-carrier mobility, electroluminescence efficiency or photovoltaic energy conversion efficiency, has presented a remarkable improvement permitting the achievement of devices with performance

compactible to commercial needs. The great advantage of semiconducting polymers compared to other electronic materials is that they are low-cost, lightweight, flexible and can be solution-processed, allowing the deposition over large areas and facilitating upscaling production.

A common characteristic of all semiconducting polymers is the chain conjugation, i.e., the alternation of single and double bonds of the carbon atoms in the backbone chain. When two carbon atoms form a double bond, three equivalent orbitals are formed due to the sp^2 hybridization and are responsible for three coplanar σ-bonds. The remaining orbital, p_z, is perpendicular to sp^2 orbitals plane and the interatomic spacing is such that an overlapping of the wave function of neighbouring electrons occurs, giving rise to a π-bond. In a conjugated structure, however, the π-electrons are delocalized over all carbon atoms along the conjugation extension, forming a set of bonding molecular orbitals (MO). The π-electrons in the highest energy occupied molecular orbital (HOMO) are more susceptible to be excited and to suffer a transition to the lowest energy unoccupied molecular orbital (LUMO) in a process commonly referred as a π-π* transition. The minimum energy necessary for the electron to undergo this transition is the energetic bandgap of the semiconducting polymer. For a more detailed study concerning the formation of molecular orbitals and electronic transitions, we recommend the studies of Kao and Hwang [1] and Pope and Swenberg [2].

An electronic π-π* transition introduces an electron in the LUMO, leaving a vacant state (hole) in the HOMO. Such transition can be thermally or optically induced, due to the absorption of a sufficiently energetic photon, in the latter case. When such transition originates an excited state characterized by an electrostatically bound electron-hole pair, it is designated as an exciton. Excitons can migrate, diffuse, dissociate or simply decay (which can be radiative or non-radiative), playing an important role in the physics of optoelectronic devices such as polymer light-emitting diodes (PLEDs) and organic photovoltaic solar cells (OPVs). Moreover, charge transport in conjugated polymers takes places via charged excited states (electrons in the LUMO or holes in the HOMO) which may be originated from exciton dissociation, charge injection from electrodes, thermal generation (intrinsic carriers), electrochemical doping, etc. In conjugated polymers with degenerate ground state, charged excited states are associated with conformational defects named solitons, whereas for polymers with non-degenerate ground state such defects are called polarons [3–5]. Polarons are half-spin semi-particles which can be negatively or positively charged, playing a similar role in conjugated polymers as electrons and holes in inorganic semiconductors or in organic molecular crystals. In the context of this chapter, we will interchange the terms for negatively (positively) charged polarons and electrons (holes) with no loss of rigor.

The schemes of the chemical structures of some conjugated polymers, frequently used as conducting/semiconducting layer of polymeric electronic/optoelectronic devices, are present-ed in **Table 1**.

From the previous exposition, we can assume that all characteristics of electronic processes of semiconducting materials such as charge injection, transport, photo-generation and recombi-nation are originated in the conjugation of the polymer backbone chain. In the following sections, we will show how these properties can be applied in electronic and optoelectronic

devices, with special focus on polymer light-emitting diodes, and discuss their basic operating mechanisms.

Polymer	Acronym	Scheme
trans-polyacetylene	*t*-PA	
Polyaniline (emeraldine base)	PANI	
Poly(3,4-ethylenedioxythiophene)	PEDOT	
Poly(*p*-phenylene vinylene)	PPV	
Poly[2-methoxy-5-(2-ethylhexyloxy)-1,4-phenylenevinylene]	MEH-PPV	
Poly(9,9-di-n-octylfluorenyl-2,7-diyl)	PFO	
Poly(3-hexylthiophene)	P3HT	

Table 1. Scheme of chemical structures of some conjugated polymers used is polymer electronic devices.

2. Polymer light-emitting diodes (PLEDs)

The first electroluminescent device with active layer based on a conjugated polymer was reported in 1990 by researchers from Cambridge University [6]. Although organic light-emitting diodes (OLEDs) with a high efficiency light output were reported 3 years before by researchers from Eastman Kodak [7], the great novelty of this work was the remarkably easy manufacturing process, based on the deposition of a thin-film, by spin-coating from a solution

of a polymer precursor onto indium-tin oxide (ITO)/glass substrates. After thermal conversion of the polymer precursor into poly(p-phenylene vinylene) (PPV), metallic electrodes (Al) were thermally evaporated on top of the polymeric film, forming a diode that, when forward polarized (ITO electrode biased positively), emitted a yellowish-green light (thanks to a bandgap energy of about 2.7 eV). Polymer light-emitting diodes (PLEDs) are, in fact, OLEDs; however, a different acronym is frequently employed to emphasize the difference whether the active layer comprises a conjugated polymer (solution processed) or a molecular solid (processed via thermal evaporation). OLEDs based on molecular solids present higher crystallinity, better thickness control, can be manufactured in multiple layers configuration and, in most of the cases, achieve higher performance than PLEDs. Nevertheless, polymers can be solution processed, allowing low-cost deposition techniques, compatibility to flexible substrates and easy expansion to large-area mass production (by means of spray or roll-to-roll deposition).

Figure 1a schematically represents the cross section of a simple, single-layer PLED structure. The 'straight-band' diagrams of **Figure 1b–e** are just a simplified vision of the formation of the metal/semiconductor junctions (which are, actually, Schottky type) at the interfaces. To obtain a PLED, it is necessary to use a high work-function (Φ_A) electrode (close to the HOMO level) as an anode and a low work-function (Φ_C) metal (close to the LUMO level) as a cathode. **Figure 1b** shows the energy diagrams for the isolated semiconductor and metallic electrodes before the contacts are made. When the device is reverse biased (ITO electrode biased negatively) or at a positive voltage lower than the difference between the electrodes' work functions divided by the elementary charge ($[\Phi_A - \Phi_C]/q$), commonly known as *built-in* voltage, V_{bi}, the barriers for the injection of electrons into the LUMO and holes into the HOMO of the conjugated polymer are very high (**Figure 1d**) and the charge-carrier transport is dominated by the thermally generated intrinsic carriers whose density is usually low, resulting in a relatively low-current device. At an external bias equal to V_{bi}, the band diagram becomes 'flat' (**Figure 1c**) and the situation is equivalent to the isolated energy levels before the formation of the junctions (**Figure 1b**). For voltages higher than V_{bi}, the band diagrams are reversed compared to the equilibrium configuration (**Figure 1d**) and the energy barriers for injection of electrons into the LUMO and holes into the HOMO are much lower, resulting in a considerably higher current device. In this situation (forward bias), electrons in the LUMO flow towards the anode and holes in the HOMO flow towards the cathode. A fraction of these injected charge carriers recombines inside the device active layer, giving origin to excitons that can undergo radiative decay, resulting in electroluminescence (EL).

A high-performance PLED is characterized by a high EL efficiency, which is mainly limited by the exciton recombination efficiency, the optical coupling device geometry and the balance in the electrode injection and bulk transport of both types (electrons and holes) of charge carriers. Each of these limiting factors in the device EL efficiency depends on several parameters demanding a thorough study. For brevity, we will focus, in the present chapter, only on the charge injection and transport processes, leaving the former two cases for further reading [8, 9].
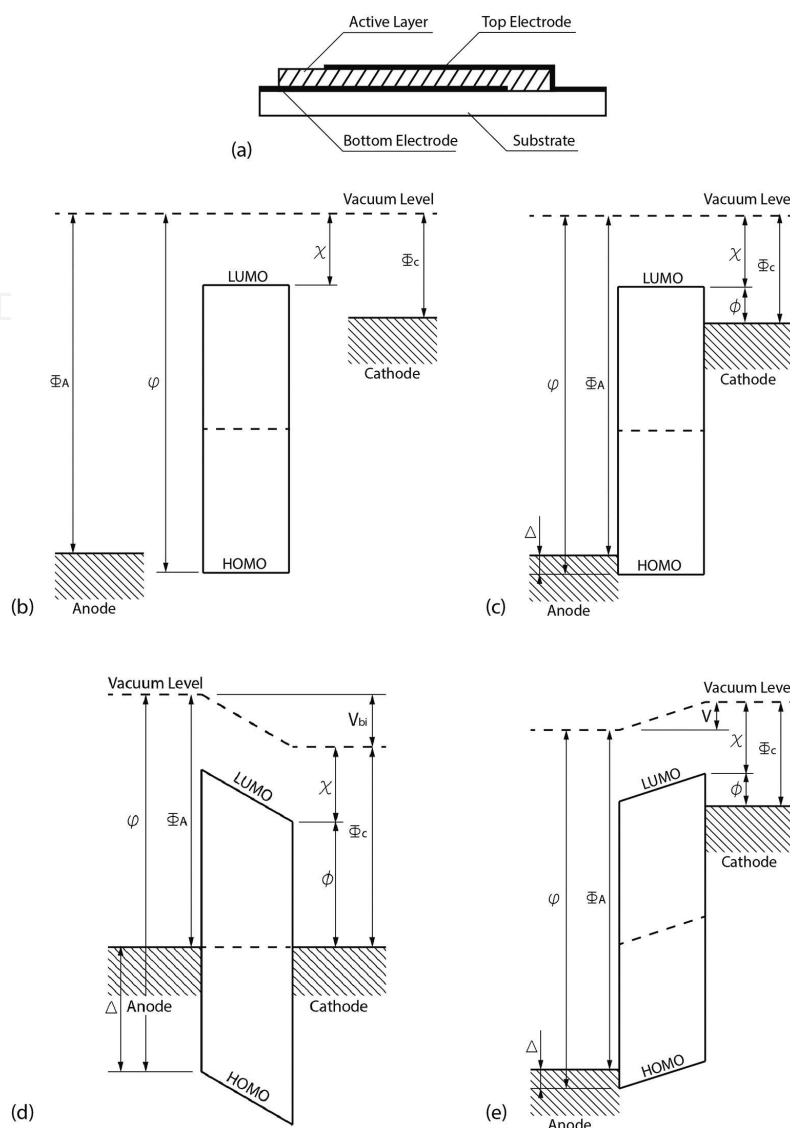
Figure 1. (a) Basic structure of a PLED; (b) energy band diagram before the contact formation; (c) 'flat-band' condition; (d) band diagram for the device in equilibrium and (e) band diagram for the device in forward bias. In these figures, Φ_A and Φ_C represents, respectively, the anode and the cathode work functions, χ, the electronic affinity, ϕ, the ionization potential of the conjugated polymer, φ and Δ, the energy barrier for injection of, respectively, electrons and holes at forward bias and V, the voltage between the device electrodes.

In an ideal PLED, electrons and holes would not have any restriction for injection from the electrodes and the density of injected charge carriers would be balanced, as well as the charge transport across the polymer layer would have equal constraints for both types of charge carriers. This picture is, though, far from being realistic. Energetic barriers need to be surpassed for the injection of electrons and holes from the electrodes into the polymeric layer, and it is virtually impossible to have equivalent injection for both electrons and holes. Although the charge injection represents a bottleneck in the current flow process, after the charge carriers are injected into the semiconducting polymer, the charge-carrier mobility becomes the decisive factor for the charge balance inside the device active layer. The charge-carrier mobility of electrons in conjugated polymers is frequently found to be several times smaller than the hole

mobility [10], which results in an asymmetric charge density distribution, strongly affecting the EL efficiency.

In a general way, the total current in a PLED can be described by

$$J \propto P_{inj} \times M_{bulk} \tag{1}$$

where P_{inj} is a function dependent on the device injection current and M_{bulk} is a function dependent on the transport current in the bulk is the transport current in the bulk. Eq. (1) means that, if the charge injection is restricted, the total device current will be limited, no matter how efficient is the charge-carrier transport in the bulk. Equivalently, if constraints in the charge-carrier transport exist, they will limit the total current in spite of how good are the electrodes for charge injection. In the following two subsections, we will present and discuss the main mechanisms that rule charge injection and transport in semiconducting polymers.

2.1. Charge-injection mechanisms in PLEDs

The ideal condition for charge injection from an electrode into a semiconducting polymer is when the work function of the cathode (Φ_C) and of the anode (Φ_A) matches, respectively, the LUMO and HOMO levels of the organic semiconductor. In such situation, when the difference between the electron affinity (χ) and the cathode work function and the ionization potential (ϕ) and the anode work function is in the order of magnitude or smaller than the thermal fluctuation energy, $k_B T$, we say that the device has ohmic contacts and that, consequently, the device current will be mainly limited by the transport in the bulk. A device with ohmic contacts does not necessarily present an ohmic behaviour, i.e., a linear dependence between current and voltage. Ohmic contacts simply mean that the barriers for charge injection from the electrodes are small enough to be neglected in the description of the total net current flowing across the device. The general case, however, is when these energy barriers for injection cannot be neglected and barriers $\varphi = \Phi_C - \chi$ for electron injection and $\Delta = \phi - \Phi_A$ for hole injection exist.
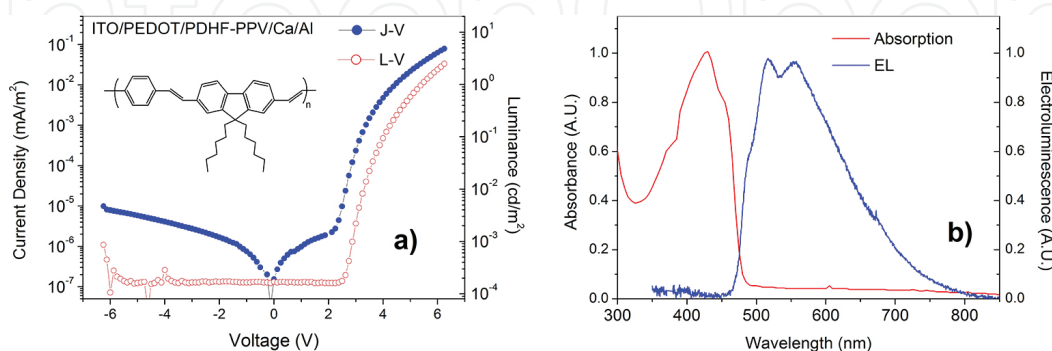
Figure 2. (a) Current-voltage (*I-V*) and luminance-voltage (*L-V*) characteristics of a typical PLED in structure ITO/PEDOT/PDHF-PPV/Ca/Al. (b) Absorption and emission (EL) spectra for the conjugated polymer used as active layer (PDHF-PPV).

Figure 2a presents the current-voltage (*I-V*) and luminance-voltage (*L-V*) characteristics of a typical PLED fabricated using a structure ITO/PEDOT/PDHF-PPV/Ca/Al. The poly(3,4-ethylenedioxythiophene), PEDOT, layer serves as a hole injection layer between the active emissive layer (made of poly (9,9–dihexyl fluorene diyl phenylene-alt-1,4-phenylene vinylene), PDHF-PPV) and the ITO electrode, providing almost ohmic contacts for hole injection into the polymer HOMO. On the other hand, the Ca electrode offers an almost ohmic contact for electron injection into the organic semiconductor LUMO. As a consequence, the onset for the forward current and for the EL device (**Figure 2a**) occurs almost simultaneously (due to balanced injection of both charge carriers) at a voltage that is nearly equal to $\Phi_A - \Phi_C/q$, and slightly above 2.0 *V*. The absorption and emission spectra of PDHF-PPV are shown in **Figure 2b**.

In a real PLED, the height of these barriers may be very different, leading to a highly unbalanced injection of electrons and holes. In such a case, the total current density will be dominated by the majority carriers, which are the most injected charge carrier type. On the other hand, the light emission will be limited by the density of injected minority charge carriers, since, for electroluminescence, both types of charge carriers are needed.

Table 2 presents some values for the ionization potential, electron affinity and energy bandgap of some conjugated polymers used in PLEDs, as well as the work function of conductive materials that can be used as electrodes. Although PEDOT is a conjugated polymer, it is highly conductive and only the value of the work function is computed **Table 2**. These data allow one to evaluate the barrier height for carrier injection in the correspondent molecular orbital (HOMO or LUMO), being essential for the design of the PLED with the desired characteristics.

	Bandgap E_g (eV)	Electron affinity χ (eV)	Ionization potential ϕ (eV)	Work function Φ (eV)
PPV	2.7	2.8	5.5	–
MEH-PPV	2.2	3.0	5.2	–
PFO	3.0	2.9	5.9	–
PEDOT	–	–	–	5.0–5.2
ITO	–	–	–	4.7–4.8
Al	–	–	–	4.06–4.41
Au	–	–	–	5.1–5.47
Ag	–	–	–	4.26–4.74
Mg	–	–	–	3.6–3.7
Ca	–	–	–	2.87–3.00

Table 2. Some values for the ionization potential, electron affinity and energy bandgap of some conjugated polymers used as active layer of PLEDs and the work function of materials commonly used as electrodes.

The device total injection current behaviour can be appropriately described by the injection properties of the lowest height energy barrier contact, in the case of highly unbalanced electron

and hole injection or, when the barrier heights at both metal/semiconductor interface are comparable to each other, by a function proportional to the sum of each separate injection current contribution.

The charge injection from an electrode into an organic semiconductor can be treated by a variety of different approaches. The first models used to explain the charge injection characteristics in PLEDs were imported and adapted from the traditional models used in inorganic semiconductor devices and insulators. However, the experimental data obtained from PLEDs can hardly be totally described by a simple model and, frequently, a combination of different processes, occurring concomitantly, is used. Another methodology, specifically developed for organic/amorphous semiconductors, includes the effects of energetic and positional disorder in the injection mechanisms. Next, we will present and discuss the most commonly used models to describe charge injection in PLEDs.

2.1.1. Injection by tunnelling

When a PLED is at forward bias (**Figure 1e**) and the energy barrier height φ (or $\varDelta$) at the metal/polymer interface cannot be neglected, one possibility for the injection of an electron (hole) into the LUMO (HOMO) is the tunnelling across this barrier. Due to the band bending caused by the external applied field, such barrier can be approximated to a triangular barrier whose width depends on the electric field. The tunnelling current density can be evaluated by considering the Wentzek-Kramers-Brillouin (WKB) approximation [1] for tunnelling through a potential given by the image force model. The analytic dependence of the current density dominated by tunnelling injection is then given by

$$J_{tu}(F) = J_0 \frac{F^2}{\phi} \exp\left(-\frac{2\alpha\phi^{3/2}}{3qF} \right)$$

(2)

where F is the electric field strength, φ is the energy barrier height at the contact, J_0 is a free fitting parameter for the current density, q is the elementary charge and $\alpha = \frac{4\pi(2m^*)^{1/2}}{h}$, where m^* is the effective mass of the charge carrier and h is the Planck constant. For a quick test if the experimental data can be fitted by Eq. (2) (and, consequently, that the major contribution to the device current is injection by tunnelling) is to make a plot of $\ln(J/F^2)$ vs. $1/F$ and expect for a linear behaviour.

An important feature of the tunnelling injection model is that it does not consider the temperature dependence on the device current, which is frequently present in PLEDs. Despite this aspect, the tunnelling injection model was successfully used to demonstrate the dependence on the barrier height and on the electric field for a complete set of experimental data obtained from devices that the metals used as electrodes, and the active layer thicknesses were systematically varied [11].

2.1.2. Current injection via thermionic emission

Another possible contribution to the injection current across an energy barrier at the semiconductor/metal interface comes from the thermionic emission of charge carriers from the electrodes. In this model, the charge carriers from the electrodes, which have enough thermal energy to overcome the energy barrier at the contact, can be injected into the LUMO/HOMO of the semiconducting polymer. The density of charge carriers which satisfies this condition follows a Boltzmann distribution $n = n_0 \exp(-\phi / k_B T)$, where n_0 is the charge-carrier density in the electrode, φ, is the energy barrier height and T, is the absolute temperature. A simple expression for the current density controlled by thermionic emission is given by

$$J_{th}(T) = AT^2 exp(-\phi / k_B T) \tag{3}$$

where A is the Richardson constant. Obviously, the effective barrier height is not constant and it depends on the electric field. Such dependence appears with the inclusion of the image force barrier lowering term, which can be considered only when the device is forward biased. The inclusion of this term results in the following effective potential in the vicinity of the injecting contact:

$$U(x, F) = \phi - \frac{q^2}{4\pi\varepsilon}\frac{1}{x} - qFx \tag{4}$$

where x represents the position from the metal/semiconductor interface and ε, is the electrical permittivity of the semiconductor. **Figure 3** shows a schematic representation of effective potential due to barrier lowering in a semiconductor/metal interface. Such potential results in an effective energy barrier height

$$\phi^* = \phi - 2\left(\frac{q^3}{4\pi\varepsilon}\right)^{\frac{1}{2}} F^{\frac{1}{2}} \tag{5}$$

which can replace the fixed barrier height in Eq. (3) to yield the thermionic emission injection current as a function dependent on temperature and electric field (or external applied voltage).

Such a barrier lowering term can also be achieved by considering a Poole-Frenkel-type effect represented by an effective barrier height

$$\phi^*(F) = \phi - aF^{\frac{1}{2}} \tag{6}$$

which gives the same functional dependence of Eq. (3) by considering a barrier height given by Eq. (5). Experimental data from PLED current-voltage curves (I-V) [12] were quite well fitted by considering such effective barrier height, but considering that the pre-factor a in Eq. (6) has a thermal activation energy, which is not initially predicted by Eq. (5).
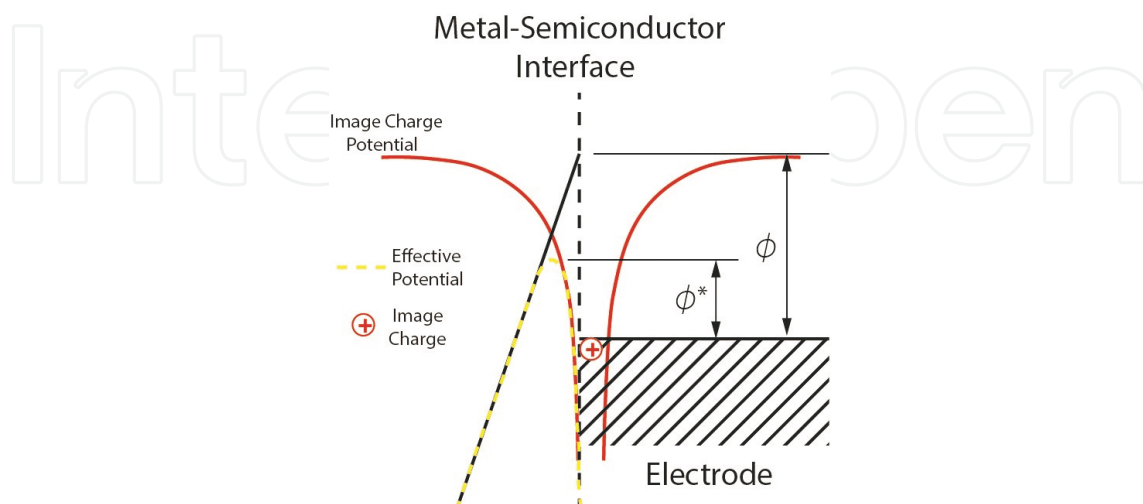
Figure 3. Schematic representation of the effective potential at a metal/semiconductor interface considering barrier lowering term due to image force effect.

2.1.3. Interface recombination effects

The charge injection problem can also be approached by using a more complete model which includes both contributions from tunnelling injection and thermionic emission, with the additional inclusion of a back flowing current contribution due to interface recombination. If one contact has a considerably higher effective energy barrier than the other, the injection current from that contact can be neglected and practically only one type of charge carrier is injected from the contacts (single-carrier device). In this situation, the charge transport in the device can be described as a combination of the continuity equation

$$\frac{\partial p(x,t)}{\partial t} + \frac{1}{q}\frac{\partial J_p(x)}{\partial x} = \Upsilon - \Omega \tag{7}$$

and a drift-diffusion form for the current density for injected holes

$$J_p = q\mu_p\left[p(x)F(x) - \frac{k_B T}{q}\frac{\partial p(x)}{\partial x} \right] \tag{8}$$

where $p(x)$ is the carrier density of holes, $F(x)$, the electric field, Υ and Ω are, respectively, the carrier generation and recombination rates and μ_p, the effective hole mobility in the organic semiconductor. The carrier mobility can also implicitly depend on temperature and electric

field. For a single-carrier device, the recombination rate term as well as the generation rate term can be evidently neglected, since we are considering organic semiconductors in the dark and with high enough bandgap energies. In Eqs. (7) and (8), the total charge inside the active layer is given by the injected charges from the electrodes and its distribution permits the evaluation of the electric field from the Poisson equation. To solve this set of equations, it is necessary to establish the boundary conditions, which are determined by the carrier currents at the interfaces. As stated in the two previous subsections, charge carriers (holes) can be injected by thermionic emission and tunnelling. Once injected in the polymer, however, holes can flow back into the metal, in a process known as interface recombination. Considering these three contributions to the current, the injection current density for holes at the contact ($x = 0$) can be represented in the form

$$J_p(0) = J_{th} + J_{tu} - J_{IR} \tag{9}$$

where J_{IR} is the interface recombination current density contribution, which is proportional to the hole density at the interface, $J_{IR} = vp(0)$. The kinetic recombination coefficient v can be determined by the detailed balance between thermionic emission and interface recombination [13–15], resulting in

$$J_p(0) = v\left\{ p_{qe}\left[F(0)\right] - p(0) \right\} + J_{tu} \tag{10}$$

where $vp(0)$ is the interface recombination current and $p_{qe}[F(0)]$ is the quasi-equilibrium carrier density at the contact, considering the electric field influence ($F(0)$) on the barrier energy lowering. Therefore, $vp_{qe}[F(0)]$ is equal to the thermionic emission current density. This equation can be solved for $p(0)$

$$p(0) = p_{qe}(F(0)) + \frac{(J_{tu} - J_d)}{v} \tag{11}$$

where J_d is the device's net current density.

The device current is commonly very small compared to the sum of the tunnelling and the thermionic emission current densities and cannot change significantly the carrier density at the semiconductor/metal interface. As a consequence, the interface recombination current density can be considered as a competition process between the tunnelling injection current density and the thermionic emission injection current density. An important feature of this model is that the magnitude of the device current density can be considerably smaller than that obtained by the direct application of thermionic emission and tunnelling injection expressions, resulting in a more realistic description of the device behaviour. A detailed discussion of this model can be found in Refs. [13–15].

Another model which considers carrier recombination in the injection current was proposed by Scott and Malliaras [16, 17], where the current injection is dependent explicitly on the charge-carrier mobility in the organic semiconductor. This model also considers that the net injection current is the result of the balance between the inflowing charge carriers and the surface recombination rate at the contact interface. Assuming that the surface recombination in a contact depends on the drift/diffusion rate of charge carriers away from the region where the image charge potential has a strong influence on the injected carriers, it is reasonable to consider that the carrier mobility plays an important role in the recombination process. The resulting injection current is

$$J_{inj} = 4\psi^2 N_0 q \mu F \exp(-\phi / k_B T) \exp(f^{1/2}) \tag{12}$$

where ψ is a function which depends smoothly on the electric field [17], N_0 is the density of states in the organic semiconductor, μ is the carrier mobility of the injected carrier at the contact, F, is the electric field strength, q, is the elementary charge and φ is the height of the Schottky barrier at the interface. The Schottky barrier lowering effect is included by the second exponential term, $f = q^3 F / \left[4\pi\epsilon (k_B T)^2 \right]$.

The advantage of this model is that it includes thermionic emission injection, image force lowering and surface recombination in a single analytic function instead of a set of differential equations coupled to balanced equilibrium equations, which is considerably convenient for fitting experimental data. This model, however, assumes that the considered carrier mobility is independent on the electric field, or that this dependence is implicit in ψ, which also has a weak dependence on F.

2.1.4. Effects of disorder in the current injection

The models for current injection presented so far were adapted from traditional models of charge injection into inorganic semiconductors. The energy barrier concepts used were, therefore, formulated by assuming the injection from the Fermi level of a metal to a continuum of delocalized states represented by the energy bands of the semiconductor (valence band for holes and conduction band for electrons). In amorphous inorganic semiconductors and organic semiconductors, due to the disorder characteristic of these materials, the electronic states available to be occupied by a charge carrier injected from the contact are better described as a distribution of localized states with a dispersion in energy. Moreover, in organic semiconductors (conjugated polymers or molecular solids), the localization of these states and their energy dispersion can be even more pronounced than in amorphous inorganic semiconductors, highlighting the influence of disorder in the charge injection and transport processes [18]. In this sense, it is reasonable to consider the use of models which include the effects of disorder to have a more realistic picture of the mechanism of charge injection into organic semiconductors.

Models considering thermally assisted tunnelling injection into localized states in a semiconducting polymer [19] and thermally limited injection current into a disordered molecular insulator via Monte Carlo simulations [20] were successfully developed to introduce the effects of disorder in the charge injection problem in organic semiconductors. A particularly interesting model, based on an analytic approach, was formulated by considering that the charge carriers are injected from the electrode into a distribution of localized hopping states in the organic semiconductor, followed by either electrode recapture or diffusion away from the attractive image potential [21].
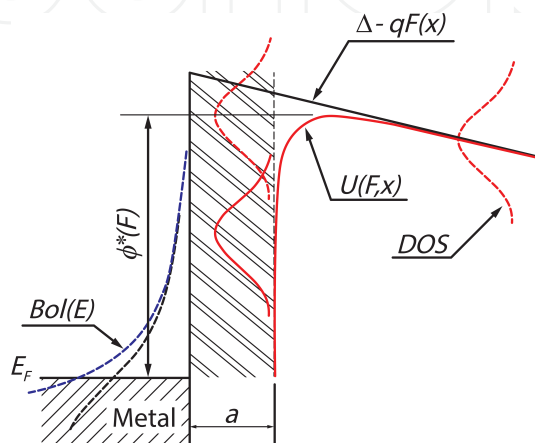
Figure 4. Representation of a metal/polymer contact in a model considering charge-carrier injection into a DOS. Dashed line Gaussian curves represent the distribution of available energy states in the semiconductor. The solid line Gaussian curve represents the first DOS after populated by an injected charge carrier, given by the convolution of the first unoccupied DOS and the edge of the Fermi distribution in the metal. The figure is adapted from Refs. [20, 21].

In this model, the initial step of the carrier injection process is the hoping from the Fermi level of an electrode, which is below the centre of the density of states (DOS) of the conjugated polymer by an energy Δ, to a localized state at a distance $x_0 \geq a$ from the interface, where a is the minimum distance between two neighbour hopping states. The potential, relative to the Fermi level of a metal, in a state of energy E, situated at a distance x from the contact, is given by

$$U\left(E,x\right) = \Delta - \frac{q^2}{16\pi\varepsilon x} - qFx + E \tag{13}$$

Once injected into a state of energy E_i, the subsequent jump of the charge carrier is towards the easiest neighbour target state of energy E_f. If $E_f > E_i$, the probability for the jump follows a Boltzmann distribution and is independent on the energy of the previous state. Such process is also valid for the first jump from the electrode to the semiconductor. For sufficiently high energy barriers, the first step is the most difficult and, therefore, limits the injection rate. The subsequent drift-diffusion process inside the polymer is considered an equilibrium process, which determines the probability of the carriers to migrate into the bulk. **Figure 4** shows a

schematic representation of the injection process from the Fermi level of a metal to an energetically and spatially disordered semiconductor.

The analytic dependence of this injection current is given by

$$J_{inj} == qv_0 \int_a^\infty dx_0 \exp(-2\gamma x_0) w_{esc}(x_0) \times \int_{-\infty}^{+\infty} dE' Bol(E') g(U_0(x) - E')$$ (14)

where $w_{esc}(x_0)$ is the probability of the carrier to avoid recombination at the interface, a, is the distance from the electrode to the first localized state, v_0, is the hopping frequency, γ, is the inverse of the carrier localization radius and the $Bol(E)$ function is defined as

$$Bol(E) = \begin{cases} \exp\left(-\dfrac{E}{k_B T}\right), E > 0 \\[2em] 1, E \leq 0 \end{cases}$$ (15)

which means that the probability of the charge carrier to jump to a higher energy state has an Arrhenius-type dependence and to jump to a lower energy state is equal to 1.

The electrostatic potential energy at a distance x from the electrode is

$$U_0(x) = \Delta - \frac{q^2}{16\pi\varepsilon x} - qFx$$ (16)

The escape probability $w_{esc}(x_0)$ at the interface can be evaluated by solving the unidimensional Fokker-Planck equation for the energy distribution given by Eq. (16). The result is

$$w_{esc}(x_0) = \frac{\int_a^{x_0} dx \exp\left[-\dfrac{q}{k_B T}\left(F_0 x + \dfrac{q}{16\pi\varepsilon}\dfrac{1}{x}\right)\right]}{\int_{-\infty}^{-\infty} dx \exp\left[-\dfrac{q}{k_B T}\left(F_0 x + \dfrac{q}{16\pi\varepsilon}\dfrac{1}{x}\right)\right]}$$ (17)

The advantage of this method as compared to the other models of charge injection into a disordered system is that it gives an analytic expression for the injection current, without the need of solving numerically a set of differential equations or performing complicated numerical simulations. **Figure 5** shows some results for the current density injected into a disordered organic semiconductor by considering Eqs. (14)–(17).

The current-density injection curves (arbitrary units) presented in **Figure 5a** were calculated at 300 K with a localization radius of 10^{-10} m, a first step distance of 0.6 nm, a dispersion of the Gaussian DOS of 80 meV and the energy barrier height Δ varying from 0.2 to 0.7 eV. In **Figure 5b**, Δ is fixed at 0.3 eV and the temperature is varied from 150 to 300 K, with all other parameters kept constant. An important feature from these results is that the current density does not have an Arrhenius dependence on the temperature, as expected from thermionic emission injection. A more detailed discussion of the results produced from this model is found in Ref. [21].
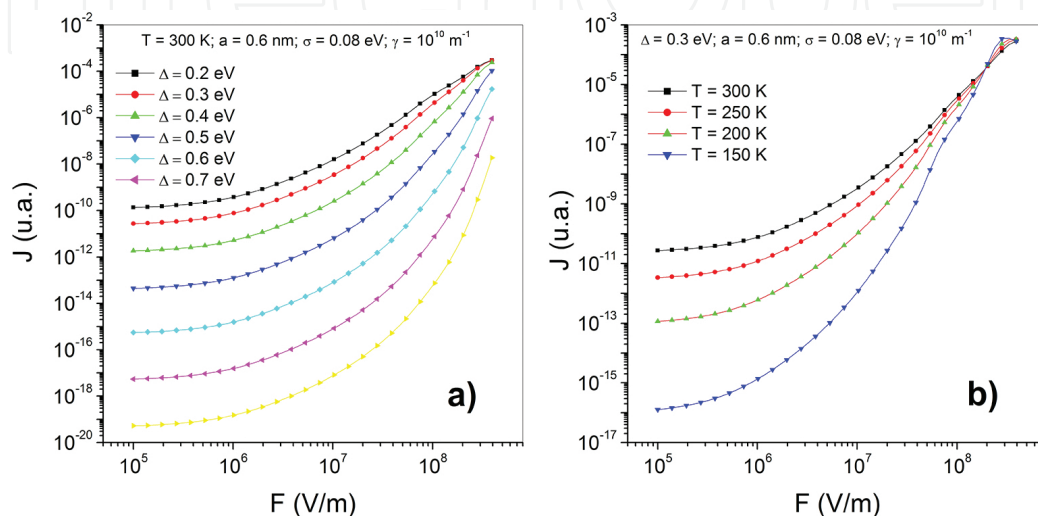
Figure 5. (a) Injection current density (arbitrary units) versus electric field simulated for different values of the zero-field energy height barrier (Δ) at 300 K. (b) Temperature dependence of the injection current density for a zero-field energy height barrier of 0.3 eV.

The model described above presents a very interesting view of the inclusion of disorder effects in the current injection from a metal into a semiconducting polymer, with evident influence on the temperature, especially in the low electric field regime. At high electric fields, the current density becomes almost independent on the temperature (**Figure 5b**), resembling a tunnelling injection dependency with, however, a very distinct functional dependence. To circumvent this problem, it is possible to conceive a model based on an electronic hopping-type injection into a DOS with the inclusion of the tunnelling probability across a triangular barrier represented by the potential at the contact interface [22]. This model considers that the carrier injection from the electrode is determined by the sum of the probabilities of each separate process to occur (hopping-type injection or tunnelling), resulting in better fitting to experimental results in a broader range of electric field and temperature. Ref. [22] is recommended for a more detailed view of this model.

2.2. Influence of the bulk transport on the current

In the previous section, we presented the most common models used to explain the current injection mechanisms in PLEDs and made a brief introduction to models which include the effects of disorder in the charge injection process. The total device current, however, depends

on Eq. (1), which means that each contribution (injection or transport in the bulk) is individually a limiting process. If the amount of charges injected from the contacts does not change significantly the density of intrinsic charge carriers, the polymer film can easily transport these charges and the injection current determines the net device current. On the other hand, if the contacts are ohmic, the polymer bulk properties will dominate the electrical behaviour of the device. Therefore, in a real device, both contributions exist and the electrical characteristics of the device are determined by which process is dominant in each regime or, if they are comparable, to a combination of both. In this section, we will focus on the main characteristics of charge transport in the bulk and on the theoretical approaches used to fit experimental data.

2.2.1. Space-charge-limited currents (SCLC)

In PLEDs, the conjugated polymer which comprises the device active emissive layer is usually in its intrinsic, non-doped form. This means that the amount of intrinsic charge carriers is considerably low (due to the relatively high bandgap) and the organic semiconductor is poorly conductive or almost an insulator. In order to achieve enough current density to promote a sufficiently visible electroluminescence, a high external electric field must be provided (above 10^6 V/m) to induce the injection of excess charge carriers into the organic semiconductor. Therefore, the operating characteristics of a PLED depend on the injection and transport of this excess charge injected in the polymer bulk. In the present subsection, we will focus on the transport characteristics of excess charge in PLEDs considering that the contacts are ohmic, i.e., they can provide as much charge as the dielectric volume can support.

For a semiconductor (or insulator) with ohmic contacts, the current due to the intrinsic charge carriers is determined by Ohm's law $J = qn\mu F$, where F is the electric field, n is the charge-carrier density in the correspondent band/molecular orbital and μ is the carrier mobility. This equation stands for single-carrier devices. For double-carrier devices, the carrier density is the sum of the densities of both charge carriers (electrons and holes), $n = n_e + n_h$, as well as the mobility is the sum of both mobilities, $\mu = \mu_e + \mu_h$. Additionally, since intrinsic charge carriers are thermally generated (geminate generation) and considering that the charge distribution is nearly uniform all over the polymer bulk, as a result from Poisson's equation, the local electric field is approximately constant, $F = V/L$, where V is the external applied voltage and L is the film thickness. Same situation occurs when the excess injected charge-carrier density is small as compared to the intrinsic charge-carrier density, resulting in a linear dependence of the device current on the applied voltage (and inverse dependence on the film thickness).

When the excess injected charge-carrier density exceeds considerably the intrinsic charge-carrier density, the local electric field is distorted and the dependence of the current on the applied voltage becomes non-linear. For a device that has an ohmic electrode for one type of charge carrier and a blocking electrode for the other, it is a good approximation to consider it a single-carrier device. If there are no charge-carrier traps in the semiconductor/insulator, the device net current is assumed to follow Mott-Gurney law [1, 23, 24]:

$$J = \frac{9}{8} \varepsilon \mu \frac{V^2}{L^3} \tag{18}$$

where ε is the electric permittivity of the semiconductor. Eq. (18) is frequently known as trap-free (SCLC) [1, 24, 25]. In this simple picture, the device current is expected to be initially linear (when the charge injection is low and the current is dominated by the intrinsic charge carriers) and becomes quadratic as space-charge effects from excess injected charge carriers surpass the amount of intrinsic charge carriers. Typical analysis uses a log-log plot of the device current (or current density) versus voltage, where the current is expected to be represented by a straight line with slope equal to 1 (linear behaviour), changing to a straight line with slope equal to 2 (quadratic dependence) when excess injected charges become dominant. Additional confirmation of the dependence denoted by Eq. (18) is the analysis of the device current against the device thickness (where an inverse cubic dependence is expected).

The quadratic dependence from Eq. (18) happens only by considering that the carrier mobility is field independent. The charge-carrier mobility in polymers, however, due to the intrinsic disorder, is generally field dependent. A commonly found field dependence [26] is

$$\mu(F) = \mu_0 \exp(\gamma \sqrt{F}) \tag{19}$$

where μ_0 is the zero-field carrier mobility and γ is a parameter which provides the temperature dependence. The device current can then be evaluated by solving the following set of equations [27]:

$$J = n(x) q \mu(F(x)) F(x) \tag{20}$$

$$\frac{\varepsilon}{q} \frac{dF(x)}{dx} = n(x) \tag{21}$$

where $n(x)$ is defined as the carrier density at position x. Assuming ohmic contacts, $n(0)$ can be estimated from the effective carrier density of states in the HOMO (for holes) or LUMO (for electrons) of the polymer and can be used as boundary condition for Eqs. (20) and (21).

Empirically, it is also observed that the zero-field carrier mobility is thermally activated [27, 28]:

$$\mu_0(T) = \mu_{T_0} \exp\left(-\frac{\Delta}{k_B T}\right) \tag{22}$$

Fitting the experimental results for each temperature by using Eqs. (20) and (21), it is also possible to find the temperature dependence of the γ parameter in Eq. (19), which is usually of the type [27, 28]:

$$\gamma(T) = \beta \left(\frac{1}{k_B T} - \frac{1}{k_B T_0} \right) \tag{23}$$

where β and T_0 are empirical parameters evaluated from the fittings.

Eqs. (19)–(23) describe the electric field and temperature dependence on the charge-carrier transport in a single-carrier, trap-free semiconductor with field-dependent carrier mobility. Such model can be quite successfully used to describe the current due to holes in PLEDs, by considering that the barrier for hole injection from ITO or ITO/PEDOT electrodes to the HOMO of the polymer is usually small (almost ohmic) and that, in conjugated polymers, holes are not strongly trapped in the bulk. In a system where the charge-carrier trap distribution is in equilibrium with the correspondent band/molecular orbital, the traps are known as shallow traps. Shallow traps do not change significantly the electric field distribution and the net effect in the charge transport can be approximated by considering an effective mobility proportional to the trap-free mobility $\mu_{\text{eff}} = \mu\theta$, where θ is independent or weakly dependent on the electric field, but dependent on the energy trap distribution [1, 24, 30–32].

Electrons, in contrast, are usually trapped in significantly deeper energy states within the energy bandgap, resulting in a much lower effective carrier mobility due to dispersive transport [29], and in a significantly non-uniform charge-carrier distribution, strongly influencing the local electric field distribution. The resulting transport current in an 'electron-only' single-carrier device can be evaluated from theories of space-charge-limited currents in an insulator with a distribution of trap states [1, 24, 30–32]. For low applied voltages, where the electron injection current is low, the intrinsic electrons dominate the charge transport, and the device current follows Ohm's law. When the excess-charge-injected carriers dominate the charge transport, the free-carrier density depends on the trap density of states that can be considered to depend exponentially on the energy:

$$n_t(E) = \left(\frac{N_t}{k_B T_t} \right) \exp \left(\frac{E - E_{\text{LUMO}}}{k_B T_t} \right) \tag{24}$$

where $n_t(E)$ is the trap density of states at energy E, E_{LUMO} is the energy of the LUMO of the polymer, N_t, is the total density of traps and $k_B T_t$ is a temperature characteristic of the trap distribution. The trap distribution of Eq. (24) results in a trap-filling-limited (TFL) current dependence that can be expressed in the form [24, 33]:

$$J = N_{LUMO} q \mu_e \left(\frac{\varepsilon}{q N_t} \right)^r \frac{V^{r+1}}{L^{2r+1}} C(r) \qquad (25)$$

where N_{LUMO} is the effective density of states in the LUMO, r is a fitting parameter defined by $r = T_t/T$ and $C(r) = r^r (2r + 1)^{r+1} (r + 1)^{-(r+2)}$. Whilst Eq. (18) gives a quadratic dependence of the current on the applied voltage and the Eqs. (19)–(23), a slight deviation from quadratic behaviour, Eq. (25) can give much steeper current dependences on the electric field. For system with deep distributions of carrier traps, the log-log plots of the J versus V curves can result in straight lines with slopes much higher than 2. Experimental results from devices, which could be approximately considered as hole-only (ITO/PPV/Au) and electron-only (Ca/PPV derivative/Ca) devices (see **Table 2** for values of work function and HOMO and LUMO energies), were fitted by these equations to corroborate the validity in the study of separate electrical transport of electrons and holes in conjugated polymers [28, 33].

For an operating PLED, however, both charge carriers (electrons and holes) must be present in the polymer bulk. Such a double-carrier device can be manufactured by using good hole- and good electron-injecting electrodes sandwiching the organic semiconductor, like a ITO/PPV/Ca structure. To model the whole device current, we cannot simply consider the independent contributions for hole (expected to be SCLC) and for electron (considered to be TFL) transport because of two additional processes which have extreme importance in double-carrier devices: charge-carrier recombination and charge neutralization. The recombination term can be considered as Langevin type, or bimolecular, where the recombination rate is proportional to the product of both electron and hole densities. The charge neutralization effect results in a net charge within the polymer bulk much lower than the actual amount of charge injected from the electrodes, permitting higher charge injection currents than in a single-carrier device. Considering field-independent mobility for electrons and holes in a trap-free semiconductor/insulator, the SCLC in the 'plasma limit' [24] is expressed by:

$$J = \left(\frac{9\pi}{8} \right)^{\frac{1}{2}} \varepsilon \left(\frac{2 q \mu_h \mu_e (\mu_h + \mu_e)}{\varepsilon B} \right)^{\frac{1}{2}} \frac{V^2}{L^3} \qquad (26)$$

where B is the bimolecular recombination constant. One important feature of Eq. (26) is that the higher the recombination, the lower the device current. Such behaviour occurs because, by increasing recombination, the amount of charge neutralization decreases. The expected dependence on the applied voltage and film thickness is, though, exactly the same for single-carrier devices in the trap-free SCLC regime. As described above, hole transport in a conjugated polymer can be considered not highly dependent on traps, but a field dependence on the carrier mobility is at least expected. Moreover, electrons are usually strongly trapped in such a way that Eq. (26) may hardly be directly applied in experimental results for PLEDs.

The inclusion of a field-dependent carrier mobility and of trapping effects in the transport mechanism of a double-carrier device complicates significantly the charge transport problem, making it impossible to find a simple analytic solution as in Eq. (26). The problem is then solved by considering that the contributions of the free charge-carrier distributions ($n_h(x)$ for holes and $n_e(x)$ for electrons) to the total device current result in [34, 35]:

$$J = q\left[\mu_h\left(F(x)\right)n_h(x) + \mu_e\left(F(x)\right)n_e(x)\right]F(x). \tag{27}$$

These free-carrier distributions are related by Poisson equation:

$$\frac{\varepsilon}{q}\frac{dF(x)}{dx} = n_h(x) - n_e(x) - n_{t,e}(x) \tag{28}$$

where $n_{t,e}(x)$ is the density of trapped electrons. The continuity equation (considering steady-state regime) is determined by the bimolecular recombination

$$\frac{1}{q}\frac{dJ_e}{dx} = -\frac{1}{q}\frac{dJ_h}{dx} = Bn_h(x)n_e(x) \tag{29}$$

In this model, holes are not considered to be significantly trapped. Moreover, Eq. (29) says that only mobile electrons contribute to charge-carrier recombination. If the contacts are ohmic, the carrier density at the interfaces can be considered as the density of states in the correspondent molecular orbitals, $n_h(x = 0) = N_{HOMO}$ and $n_e(x = L) = N_{LUMO}$ (the hole-injecting electrode is at $x = 0$). These conditions are used as boundary conditions to find the solution of Eqs. (27)–(29). The field and temperature dependence of the carrier mobility is provided by Eqs. (19), (22) and (23). By considering the exponential distribution of traps for electrons from Eq. (24), it is possible to obtain the density of trapped electrons

$$n_{t,e}\left(x\right) = N_t\left[\frac{n_e(x)}{N_{LUMO}}\right]^{T/T_t} \tag{30}$$

To properly determine the current characteristics of a double-carrier device using the above equations, one must first produce and characterize hole-only [27] and electron-only [33] devices, varying the temperature and device thickness in order to obtain the needed parameters from Eqs. (22) and (23) (for holes) and (24) and (25) (for electrons). Therefore, Eqs. (27)–(29) can be solved numerically by considering Eq. (30), with the bimolecular constant B as the unknown parameter to be determined. This procedure was applied in the fitting of experi-

mental data of double-carrier devices, in order to find optimum mobility values for PLED performance [35, 36].

2.2.2. Effects of disorder in the charge-carrier transport

The previous subsection presented a discussion on how the effects of space-charges in the bulk affect the charge-carrier transport and, consequently, the device current in dc current-voltage measurements. The models considered, though, a field-independent mobility (which is hardly found in organic semiconductors) or an empirical temperature and local electric field dependence resembling a Poole-Frenkel behaviour, represented by the combination of Eqs. (19), (22) and (23),

$$\mu(T,F) = \mu_{T_0} \exp\left(-\frac{\Delta}{k_{\mathrm{B}}T}\right) \exp\left[\beta F^{1/2}\left(\frac{1}{k_{\mathrm{B}}T} - \frac{1}{k_{\mathrm{B}}T_0}\right)\right] \tag{31}$$

Despite the relatively good consistency with experimental results, the arguments used to justify such dependence are still controversial. The Poole-Frenkel behaviour is considered as a consequence of the electric field lowering of the potential barrier that a carrier needs to overcome to leave a charged centre. An argument against the attribution of the mobility dependence to Poole-Frenkel effect is that such behaviour is observed in a large variety of materials which, in most of the cases, the amount of charged traps in the bulk can be considered negligible.

A more reasonable consideration is that such dependence comes from the disorder inherent of organic semiconductors. The charge transport mechanism in these materials is then associated with the hopping of carriers within a randomly positioned and energetically disordered system of localized states [2, 37]. Most of the models which consider hopping between localized states are based on Miller-Abrahams expression [38] for the probability of a tunnelling carrier jump over a distance r separating an initial state at energy E_i and a final state at energy E_f, written as

$$P(r, E_i, E_f) = \nu_0 \exp(-\gamma r) \times \begin{cases} \exp\left(-\frac{E_f - E_i}{k_{\mathrm{B}}T}\right), E_f > E_i \\ \\ 1, E_f < E_i \end{cases} \tag{32}$$

where γ is the inverse of the localization radius of the electronic wavefunction and ν_0, is the attempt-to-jump frequency. The spatial dependence from Eq. (32) says that the carrier jump rate decreases exponentially with increasing distance between hopping sites. Moreover, the symmetry on position means that forward or backward jumps are equally probable and,

therefore, within a hypothetic system where all hopping sites have the same energy, the trapping and releasing rates would be equal. On the other hand, the energetic dependence is not symmetrical. Upward jumps are thermally activated, whereas downward jumps dissipate the excess energy in the form of phonon emission. The consequence is that the upward jumps are much slower than downward jumps, resulting in totally different trapping and releasing rates for forward and backward jumps between two fixed states at different energy levels. The introduction of energetic disorder in a localized states hopping system, therefore, influences strongly the carrier transport behaviour.

The analytic treatment of carrier hopping in such a system described above can be quite complicated, since it is virtually impossible to consider the evaluation of all possible spatial and energetic configurations. However, approximate methods for a simplified picture of the problem are frequently applied. A particularly efficient method is based on the effective transport level [39], which effectively reduces the problem of hopping within a spatially and energetically disordered system into a trap-controlled transport mechanism.

Analytic models considering the random hopping of the carrier within an energetically and positionally disordered system were formulated to study the concentration and temperature dependence of the carrier mobility considering an arbitrary DOS distribution and in the high density of carriers regime [40, 41]. However, the direct application of the results to the set of equations of SCLC in Section 2.2.1 is still quite limited. Models based on Monte Carlo simulations were used to introduce the concept of spatially correlated energetic disorder in a system, assuming a Gaussian DOS distribution [42–44]. The results show that the obtained dependence of the carrier mobility on the electric field resembles the Poole-Frenkel-type behaviour in a quite wide electric field range.

3. Conclusion

The basic models of the operating mechanisms of PLEDs presented in this chapter can be employed in the interpretation of experimental results from dc electrical characterization of PLEDs, allowing the extraction of intrinsic polymer parameters like charge carrier mobility or structure-dependent parameters like the energy barrier height at a contact. To properly investigate the results from the electrical characterization of a PLED, however, a critical analysis procedure must be considered. First of all, knowledge of the undistorted energy bands of the polymer and the work function of the contacts is needed. From these information, it is possible to know if the assumption of ohmic contacts considered for a SCLC analysis is valid or not. If the contacts are not ohmic, a combined contribution from thermally activated injection and tunnelling must be considered and used to give the actual boundary conditions for the carrier density at the contacts. If thermionic emission and tunnelling cannot provide the necessary functional injection current, it can be estimated from the presented models considering interface recombination or spatial and energetic disorder in the first carrier jump in the semiconductor. For modelling a double-carrier device, where bimolecular recombination effects take place, the ideal approach is to first analyse, separately, the electrical transport in

both single-carrier devices (electron-only and hole-only), with metallic electrodes as close as possible to the ohmic contact condition. Models considering spatial and energetic disorder in the polymer bulk, though are more accurate and complete from the theoretical viewpoint, are still difficult to be directly applied to the fitting of experimental dc current-voltage curves, being not applicable to all operating regimes.

Acknowledgements

Author details

Lucas Fugikawa Santos[1*] and Giovani Gozzi[2]

*Address all correspondence to: lucas@sjrp.unesp.br

1 Physics Department, Campus of São José do Rio Preto, State University of São Paulo–UNESP, São Paulo, Brazil

2 Physics Department, Campus of Rio Claro, State University of São Paulo–UNESP, São Paulo, Brazil

References

[1] Kao K.C.; Hwang W. Electrical Transport in Solids, With Particular Reference to Organic Semiconductors (International Series in the Science of the Solid States). 1st ed. Oxford: Pergamon Press; 1981. 660 pp.

[2] Pope M.; Swenberg C.E. Electronic Processes in Organic Crystals and Polymers. 2nd ed. Oxford: Oxford University Press; 1999. 1328 pp.

[3] Su W.P.; Schrieffer J.R.; Heeger A.J. Solitons in polyacetylene. Physical Review Letters. 1979;42(25):1698–1701. DOI: 10.1103/PhysRevLett.42.1698

[4] Su W.P.; Schrieffer J.R.; Heeger A.J. Solitons in polyacetylene. Physical Review B. 1980;22(4):2099–2111. DOI: 10.1103/PhysRevB.22.2099

[5] Heeger A.J.; Kivelson S.; Schrieffer J.R.; Su W.P. Solitons in conducting polymers. Reviews of Modern Physics. 1998;60(3):781–851. DOI: 10.1103/RevModPhys.60.781

[6]   Burroughes J.H.; Bradley D.D.C.; Brown A.R.; Marks R.N.; Mackay K.; Friend R.H.; Burns P.L.; Holmes A.B. Light-emitting diodes based on conjugated polymers. Nature. 1990;347(6293):539–541. DOI: 10.1038/347539a0

[7]   Tang C.W.; VanSlyke S.A. Organic electroluminescent diodes. Applied Physics Letters. 1987;51(12):913–915. DOI: 10.1063/1.98799

[8]   Tsutsui T.; Takada N. Progress in emission efficiency of organic light-emitting diodes: basic understanding and its technical application. Japanese Journal of Applied Physics. 2013;52:110001. DOI: 10.7567/JJAP.52.110001

[9]   Gather M.C.; Reineke S. Recent advances in light outcoupling from white organic light-emitting diodes. Journal of Photonics for Energy. 2015;5:057607. DOI: 10.1117/1.JPE. 5.057607

[10] Lu C.; Pi S.; Meng H. Effect of defect-enhanced molecular oxygen adsorption on the imbalance of hole versus electron mobility in conjugated polymers. Physical Review B. 2007;75(19):195206. DOI: 10.1103/PhysRevB.75.195206

[11] Parker I.D. Carrier tunneling and device characteristics in polymer light-emitting diodes. Journal of Applied Physics. 1994;75(3):1656–1666. DOI: 10.1063/1.356350

[12] Santos L.F.; Bianchi R.F.; Faria R.M. Electrical properties of polymeric light-emitting diodes. Journal of Non-Crystalline Solids. 2004;338–340(1 Spec. Iss.):590–594. DOI: 10.1016/j.jnoncrysol.2004.03.048

[13] Campbell I.H.; Smith D.L. Physics of polymer light emitting diodes. In: Hadziioannou, G.; van Hutten, P.F., editors. Semiconducting Polymers. 1st ed. Weinheim: Willey-VCH; 2000. pp. 333–364.

[14] Davids P.S.; Campbell I.H.; Smith D.L. Device model for single carrier organic diodes. Journal of Applied Physics. 1997;82(12):6319–6325. DOI: 10.1063/1.366522

[15] Crone B.K.; Campbell I.H.; Davids P.S.; Smith D.L. Charge injection and transport in single-layer organic light-emitting diodes. Applied Physics Letters. 1998;73(21):3162–3164. DOI: 10.1063/1.122706

[16] Malliaras G.G.; Scott J.C. The roles of injection and mobility in organic light emitting diodes. Journal of Applied Physics. 1998;83(10):5399–5403. DOI: 10.1063/1.367369

[17] Scott J.C.; Malliaras G.G. Charge injection and recombination at the metal-organic interface. Chemical Physics Letters. 1999;299(2):115–119. DOI: 10.1016/S0009-2614(98)01277-9

[18] da Silva Filho D.A.; Olivier Y.; Coropceanu V.; Brédas J.L.; Cornil J. Theoretical aspects of charge transport in organic semiconductors. In: Bao, Z.; Locklin, J., editors. Organic Field Effect Transistors. 1st ed. Boca Raton: CRC Press Taylor and Francis; 2007. pp. 1–72.

[19] Abkowitz M.A.; Mizes H.A.; Facci J.S. Emission limited injection by thermally assisted tunneling into a trap-free transport polymer. Applied Physics Letters. 1995;66(10):1288–1290. DOI: 10.1063/1.113272

[20] Gartstein Y.N.; Conwell E.M. Field-dependent thermal injection into a disordered molecular insulator. Chemical Physics Letters. 1996;255(1–3):93–98. DOI: 10.1016/0009-2614(96)00359-4

[21] Arkhipov V.I.; Emelianova E.V.; Tak Y.H.; Bässler H. Charge injection into light-emitting diodes: theory and experiment. Journal of Applied Physics. 1998;84(2):848. DOI: 10.1063/1.368146

[22] Gozzi G.; Queiroz E.L.; Zucolotto V.; Faria R.M. Hopping–tunneling model to describe electric charge injection at metal/organic semiconductor heterojunctions. Physica Status Solidi (B). 2015;252(2):404–410. DOI: 10.1002/pssb.201451556

[23] Mott N.F.; Gurney R.W. Electronic Process in Ionic Crystals. 2nd ed. Oxford: Oxford University Press; 1948. 275 p.

[24] Lampert M.A.; Mark P. Current Injection in Solids. 1st ed. New York: New York Academic Press; 1970. 351 p.

[25] Parmenter R.H.; Ruppel W. Two-carrier space-charge-limited current in a trap-free insulator. Journal of Applied Physics. 1959;30(10):1548–1558. DOI: 10.1063/1.1734999

[26] Pai D.M. Transient photoconductivity in poly(N-vinylcarbazole). Journal of Chemical Physics. 1970;52(5):2285–2291. DOI: 10.1063/1.1673300

[27] Blom P.W.M.; de Jong M.J.M.; van Munster M.G. Electric-field and temperature dependence of the hole mobility in poly(p-phenylene vinylene). Physical Review B. 1997;55(2):R656–R659. DOI: 10.1103/PhysRevB.55.R656

[28] Gill W.D.; Kanazawa K.K. Transient photocurrent for field-dependent mobilities. Journal of Applied Physics. 1972;43(2):529–534. DOI: 10.1063/1.1661151

[29] Santos L.F.; Faria R.M.; de Andrade A.R.; Faria G.C.; Amorin C.A.; Mergulhao S. Transition from dispersive to non-dispersive transport of holes in poly(2-methoxy-5-(2′-ethyl-hexyloxy)-1,4-phenylene vinylene) light-emitting diodes investigated by time of flight measurements. Thin Solid Films. 2007;515(20–21):8034–8039. DOI: 10.1016/j.tsf.2007.03.052

[30] Rose A. Space-charge-limited currents in solids. Physical Review. 1955;97(6):1538–1544.

[31] Lampert M.A. Simplified theory of space-charge-limited currents in an insulator with traps. Physical Review. 1956;103(6):1648–1656. DOI: 10.1103/PhysRev.103.1648

[32] Mark P.; Helfrich W. Space-charge-limited currents in organic crystals. Journal of Applied Physics. 1962;33(1):205–215. DOI: 10.1063/1.1728487

[33] Blom P.W.M.; de Jong M.J.M.; Vleggaar J.J.M. Electron and hole transport in poly(p-phenylene vinylene) devices. Applied Physics Letters. 1996;68(23):3308–3310. DOI: 10.1063/1.116583

[34] Blom P.W.M.; de Jong M.J.M.; Breedijk S. Temperature dependent electron-hole recombination in polymer light-emitting diodes. Applied Physics Letters. 1997;71(7): 930–932. DOI: 10.1063/1.119692

[35] Blom P.W.M.; de Jong M.J.M. Electrical characterization of polymer light-emitting diodes. IEEE Journal of Selected Topics in Quantum Electronics. 1998;4(2):105–112. DOI: 10.1109/2944.669477

[36] Blom P.W.M.; Vissenberg M.C.J.M.; Huiberts J.N.; Martens H.C.F.; Schoo H.F.M. Optimum charge-carrier mobility for a polymer light-emitting diode. Applied Physics Letters. 2000;77(13):2057–2059. DOI: 10.1063/1.1313254

[37] Bässler H. Charge transport in disordered organic photoconductors – a monte-carlo simulation study. Physica Status Solidi B. 1993;175(1):15–56. DOI: 10.1002/pssb.2221750102

[38] Miller A.; Abrahams E. Impurity conduction at low concentrations. Physical Review. 1960;120(3):745–755. DOI: 10.1103/PhysRev.120.745

[39] Monroe D. Hopping in exponential band tails. Physical Review Letters. 1985;54(2):146–149. DOI: 10.1103/PhysRevLett.54.146

[40] Arkhipov V.I.; Heremans P.; Emelianova E.V.; Adriaenssens G.J.; Bassler H. Weak-field carrier hopping in disordered organic semiconductors: the effects of deep traps and partly filled density-of-states distribution. Journal of Physics-Condensed Matter. 2002;14(42):9899–9911. DOI: 10.1088/0953-8984/14/42/305

[41] Arkhipov V.I.; Emelianova E.V.; Heremans P.; Adriaenssens G.J. Equilibrium hopping conductivity in disordered materials. Journal of Optoelectronics and Advanced Materials. 2002;4(3):425–436.

[42] Gartstein Y.N.; Conwell E.M. High-field hopping mobility in molecular-systems with spatially correlated energetic disorder. Chemical Physics Letters. 1995;245(4–5):351–358. DOI: 10.1016/0009-2614(95)01031-4

[43] Gartstein Y.N.; Conwell E.M. Off-diagonal disorder and activation-energy of high-field hopping motion. Physical Review B. 1995;51(11):6947–6952. DOI: 10.1103/PhysRevB.51.6947

[44] Rakhmanova S.V.; Conwell E.M. Mobility variation with field in conducting polymer films. Synthetic Metals. 2001;116(1–3):389–391. DOI: 10.1016/S0379-6779(00)00443-4